

A* Orthogonal Matching Pursuit: Best-First Search for Compressed Sensing Signal Recovery

Nazim Burak Karahanoglu^{a,b,*}, Hakan Erdogan^a

^a*Department of Electronics Engineering, Sabanci University, Istanbul 34956, Turkey*

^b*Information Technologies Institute, TUBITAK-BILGEM, Kocaeli 41470, Turkey*

Abstract

Compressed sensing aims at reconstruction of sparse signals following acquisition in reduced dimensions, which makes the recovery process under-determined. Due to sparsity, required solution becomes the one with minimum ℓ_0 norm, which is untractable to solve for. Commonly used reconstruction techniques include ℓ_1 norm minimization and greedy algorithms. This manuscript proposes a novel semi-greedy approach, namely A* Orthogonal Matching Pursuit (A*OMP), which performs A* search for the sparsest solution on a tree whose paths grow similar to the Orthogonal Matching Pursuit (OMP) algorithm. Paths on the tree are evaluated according to an auxiliary cost function, which should compensate for different path lengths. For this purpose, we suggest three different structures. We show that novel dynamic cost functions provide improved results as compared to a conventional choice. Finally, we provide reconstruction results on both synthetically generated data and images showing that A*OMP outperforms well-known CS reconstruction methods, Basis Pursuit (BP), OMP and Subspace Pursuit (SP).

Keywords: compressed sensing, sparse signal reconstruction, orthogonal matching pursuit, best-first search, A* search, auxiliary functions for A* search

1. Introduction

Representations of sparse signals in compressed forms have been of great interest in the signal processing community. Standard transform coding methods require acquisition of the signal in full dimensions, even though the signal is sparse and dimensionality reduction can only be obtained by neglecting small coefficients after transformation of the signal. Compressed sensing (CS), in contrast, deals with acquisition of sparse signals directly in reduced dimensions, which necessitates solution of an ill-posed recovery problem to get the original signal back. CS recovery is based on the following question: Can a reduced number of observations (less than Shannon-Nyquist rate) contain enough information for exact reconstruction of sparse signals? This might seem quite unnatural, however CS literature, *i.e.* [1], [2] and [3], states that it is indeed possible under certain assumptions.

Exact solution of the CS reconstruction problem requires solution of an ℓ_0 minimization problem, which is unpractical. One of the solutions that can be found in the literature is the Basis

*Corresponding author

Email addresses: karahanoglu@sabanciuniv.edu (Nazim Burak Karahanoglu), herdogan@sabanciuniv.edu (Hakan Erdogan)

Pursuit [4], which replaces ℓ_0 minimization problem with an ℓ_1 minimization, which can be solved by linear programming. Another family of algorithms, so called greedy pursuits, such as Matching Pursuit (MP) [5], Orthogonal MP (OMP) [6], regularized OMP (ROMP) [7], Subspace Pursuit (SP) [8], Compressive Sampling MP (CoSaMP) [9] and etc, find approximate solutions by solving a stage-wise constrained residue minimization problem.

This manuscript details a novel semi-greedy approach, namely A* Orthogonal Matching Pursuit (A*OMP), that incorporates the A* Search [10, 11, 12, 13, 14], a best-first search technique that is frequently used in path finding, graph traversal and speech recognition, with OMP. A preliminary and summary version of this work has been presented in [15]. This paper serves the purpose of a deeper and complete introduction of A*OMP and a broader evaluation.

A*OMP algorithm proposes to solve the reconstruction problem with an A* search that employs the OMP algorithm at each branch of the search tree. By utilizing best-first search, multiple paths can be evaluated during the search instead of the single path structures of other algorithms such as MP or OMP. By selection of appropriate auxiliary cost functions to compensate different path lengths, A* search enables statewide residue minimization in an intelligent manner over multiple candidates. We introduce two new dynamic auxiliary functions which are different than the trivial additive one. These dynamic auxiliary functions provide improved accuracies in simulated 1D signal reconstructions. The introduced methods provide lower normalized mean squared errors than other methods when nonzero coefficients of the sparse signals are chosen to be uniformly or normally distributed. The performance of the new algorithms are better than the competitors for compressed sensing reconstructions of natural images as well.

The rest of this manuscript is organized as follows: First, compressed sensing reconstruction problem and some of the existing solutions are discussed briefly in sections 2 through 4. We introduce A* search in section 5. In section 6, the proposed A*OMP algorithm is described in detail along with novel cost functions. Before concluding, we demonstrate the reconstruction performance of A*OMP in comparison to BP, SP and OMP algorithms in section 7. These demonstrations include reconstruction of not only synthetically generated data, but also well-known images. Finally, the manuscript is concluded with a short summary of the work and discussion of the results.

2. Compressed Sensing

2.1. Problem Definition

Let us consider a signal \mathbf{x} which has a K -sparse representation in the (orthonormal) basis Ψ :

$$\mathbf{x} = \Psi\alpha, \quad (1)$$

where $\mathbf{x}, \alpha \in \mathbb{R}^N$, $\Psi \in \mathbb{R}^{N \times N}$, $\|\alpha\|_0 = K$ and $K < N$.

CS aims at representing the signal \mathbf{x} with $M < N$ observations, which are obtained via the $M \times N$ observation matrix, or measurement basis, Φ :

$$\mathbf{y} = \Phi\mathbf{x} = \Phi\Psi\alpha. \quad (2)$$

Following [16], we define the holographic basis as $\mathbf{V} = \Phi\Psi$, which is of $M \times N$. As $M < N$, solving for α directly from (2) is ill-posed: There exist multiple solutions which are shifted versions of the sparsest solution α in the null-space of the holographic basis.

In CS theory, the reconstruction problem is formulated as an ℓ_0 minimization by incorporating the sparsity of the signal \mathbf{x} in Ψ :

$$\alpha = \arg \min \|\alpha\|_0 \quad s.t. \quad \mathbf{y} = \Phi \mathbf{x} = \mathbf{V} \alpha. \quad (3)$$

Direct solution of (3) requires an exhaustive combinatorial search over all subsets of the columns of \mathbf{V} [1, 17]. Thus, it is not feasible even for signals that are moderate in size.

2.2. Major Families of Algorithms for Sparse Signal Reconstruction

A variety of solution strategies have emerged in the CS field for solving (3). Following Tropp, [18], the major approaches can be categorized into at least five classes, which are listed as greedy pursuit algorithms, convex relaxation, Bayesian framework, nonconvex optimization and brute force methods. In this work, we are interested in the first two categories:

1. Convex (ℓ_1) relaxation cast the ℓ_0 minimization into an equivalent ℓ_1 minimization problem whose solution is tractable. This concept was first introduced in BP [19, 4].
2. Greedy pursuit algorithms employ search mechanisms which refine a sparse solution iteratively. MP [5] aims at obtaining the sparse representation sequentially, starting from a null representation and expanding it at each step by a scaled version of a selected basis vector. Some extensions of this idea, such as OMP [6], ROMP [7], SP [8], CoSaMP [9] can be found in the literature.

2.3. Theoretical Guarantees - The Restricted Isometry Property

Obtaining theoretical guarantees for exact recovery is an important topic in compressed sensing community. An important means for this purpose is the restricted isometry property (RIP) [20, 3, 21], which allows theoretical guarantees for many algorithms.

For simplicity, let's assume \mathbf{x} is sparse itself, or equivalently $\Psi = \mathbf{I}$. Then, the holographic basis becomes equal to the observation matrix, $\mathbf{V} = \Phi$. We, now, summarize RIP for Φ , while the results still remain valid for different choices of Ψ such as wavelet or Discrete Cosine Transform (DCT) basis, if the observation matrix is chosen appropriately.

Given Φ , two requirements are crucial for exact reconstruction of K -sparse \mathbf{x} [18]

- i) **Uniqueness:** Each observed signal \mathbf{y} should have a unique K -sparse representation \mathbf{x} in Φ . It can easily be shown that uniqueness requires all subsets containing $2K$ column vectors of Φ to be linearly independent.
- ii) **Stability:** Each observed signal \mathbf{y} should be stably determined. That is, the magnitudes of \mathbf{y} and \mathbf{x} should be comparable.

These requirements are ensured by the RIP which is defined as follows: The matrix Φ is said to satisfy the K-RIP if there exists a restricted isometry constant δ_K , $0 < \delta_K < 1$ such that

$$(1 - \delta_K) \|\mathbf{x}\|_2^2 \leq \|\Phi \mathbf{x}\|_2^2 \leq (1 + \delta_K) \|\mathbf{x}\|_2^2, \forall \mathbf{x} : \|\mathbf{x}\|_0 \leq K. \quad (4)$$

The nature of the RIP can be better understood by the uniqueness requirement: A system satisfying the RIP acts almost like an orthonormal system for sparse linear combinations of its columns [20], making reconstruction of sparse signals from lower dimensional observations possible.

Analysis in [3] state that random matrices with independent and identically distributed (i.i.d.) entries following Gaussian or Bernoulli distributions satisfy the RIP with high probabilities if

$$K \approx C \frac{M}{\log(N/M)}, \quad (5)$$

where C depends on the restricted isometry constant δ_K . On the other hand, in case the observation matrix is randomly selected from discrete Fourier transform, a weaker RIP bound is obtained:

$$K \approx C \frac{M}{\log N^6}. \quad (6)$$

With respect to these bounds, random observation matrices can provide more compact representations of sparse signals, which is the motivation for their frequent use in compressed sensing.

3. Convex Relaxation

This important family of sparse signal reconstruction algorithms rely on the relaxation of (3) by replacing the ℓ_0 norm minimization with an ℓ_1 norm, which first appeared in Basis Pursuit [4]. In this context, (3) is translated into the following ℓ_1 minimization problem:

$$\alpha = \arg \min \|\alpha\|_1 \quad s.t. \quad \mathbf{y} = \mathbf{V}\alpha. \quad (7)$$

This translation of the problem makes the solution possible via computationally tractable convex optimization methods, such as pivoting, linear programming and gradient methods [18].

Among ℓ_1 optimization methods, Basis Pursuit is based on solving (7) by linear programming (LP) techniques. Employing well known LP techniques, this problem can be solved in polynomial time [16]. The LP-equivalent of (7), discussion of simplex and interior point methods for BP and details of the algorithm can be found in [4].

The RIP plays an important role in the applicability of the ℓ_1 relaxation in the original ℓ_0 norm minimization problem. Extensive analysis of the necessary RIP conditions for the ℓ_1 relaxation are provided by [20, 3, 21]. These demonstrate that the ℓ_0 and ℓ_1 minimizations lead to the same K -sparse representation if the observation matrix satisfies RIP with $\delta_{2K} < \sqrt{2} - 1$.

4. Greedy Pursuit Algorithms

4.1. Matching Pursuit

Matching Pursuit (MP) [5] is historically the first greedy algorithm that aims iterative recovery of the K -sparse representation α . Each iteration of MP tends to recover one of the non-zero entries in α . It selects the basis vector (among columns of \mathbf{V}) which best matches the approximation error (residue) of the last iteration and adds a scaled version of it to the approximation of \mathbf{y} . The iterations are carried on until a specific termination criterion is achieved.

Let $v_n \in \mathbb{R}^M, n = 1, 2, \dots, N$ show the (linearly dependent) basis vectors in the holographic basis $\mathbf{V} = \mathbf{\Phi}\mathbf{\Psi}$. We define \mathbf{s}^l as the selected basis vector at iteration l and c^l as the corresponding coefficient. $\hat{\mathbf{y}}$ and $\hat{\alpha}$ denote the approximations of \mathbf{y} and α . \mathbf{r}^l is the residue after the l 'th iteration. \mathbf{S} and \mathbf{c} denote the matrix (or, exchangeably in context, the set) of basis vectors selected from \mathbf{V} for representing \mathbf{y} and the vector of corresponding coefficients respectively. Note that, in this notation, superscripts always represent the number of vectors in the selected basis, which for now

is equal to the number of iterations. This choice was made on purpose and subscripts will be used in next sections for differentiating between paths in A*OMP discussion.

Using this representation, the approximation of the observation vector and the residue after L iterations are written as

$$\begin{aligned}\hat{\mathbf{y}} &= \sum_{l=1}^L c^l \mathbf{s}^l = \mathbf{S} \mathbf{c}, \\ \mathbf{r}^L &= \mathbf{y} - \hat{\mathbf{y}} = \mathbf{y} - \sum_{l=1}^L c^l \mathbf{s}^l.\end{aligned}\tag{8}$$

Now, we can continue with the algorithm itself. The parameters are initialized as follows:

$$\hat{\mathbf{y}} = \mathbf{0}, \hat{\alpha} = \mathbf{0}, \mathbf{r}^0 = \mathbf{y}, \mathbf{S} = \{\}, \mathbf{c} = \mathbf{0}.\tag{9}$$

At iteration l , we select the basis vector that best matches the residue of the previous step

$$\mathbf{s}^l = \arg \max_{\mathbf{v}_n \in \mathbf{V} \setminus \mathbf{S}} \langle \mathbf{r}^{l-1}, \mathbf{v}_n \rangle,\tag{10}$$

and add it to the set of selected vectors

$$\mathbf{S} = \mathbf{S} \cup \mathbf{s}^l.\tag{11}$$

The corresponding coefficient c^l is selected as

$$c^l = \langle \mathbf{r}^{l-1}, \mathbf{s}^l \rangle,\tag{12}$$

and the residue becomes

$$\mathbf{r}^l = \mathbf{r}^{l-1} - c^l \mathbf{s}^l.\tag{13}$$

The algorithm will continue iterations until a specified termination criterion is satisfied. One possibility is to terminate iterations when the residue reaches a lower bound as in the original MP paper [5]. We, however, fix the number of iterations as K in this work in order to compare the MP algorithm to our proposal.

(8) can be utilized to obtain an approximation of \mathbf{y} at this level. This will, however, not be the optimal result, as the correlations between selected basis vectors are not considered during the calculation of c^l 's. Hence \mathbf{r}^K , in general, will not be orthogonal to \mathbf{S} . The coefficients should be corrected by orthogonal projection of \mathbf{r}^K onto \mathbf{S} :

$$\begin{aligned}\hat{\epsilon} &= \arg \min_{\epsilon \in \mathbb{R}^K} \| \mathbf{r}^K - \mathbf{S} \epsilon \|_2, \\ \mathbf{c} &= \mathbf{c} + \hat{\epsilon}.\end{aligned}\tag{14}$$

Approximation of α is obtained by mapping \mathbf{c} onto $\hat{\alpha}$ where the locations of nonzero entries are provided by the set \mathbf{S} . Finally, we obtain the reconstructed vector $\hat{\mathbf{x}}$ as

$$\hat{\mathbf{x}} = \Psi \hat{\alpha}.\tag{15}$$

Although MP employs a final orthogonal projection step, internal iterations are still suboptimal as they do not take into account the non-orthogonality of the basis vectors. After an internal iteration, the residue is not necessarily orthogonal to the selected basis, therefore the following iteration is subject to choosing a suboptimal basis vector. These suboptimal choices due to the non-orthogonality of the basis vectors make MP fail often.

4.2. Orthogonal Matching Pursuit

In order to improve the performance of MP in overcomplex dictionaries, a number of extensions have been suggested. One of the best known extensions is the Orthogonal Matching Pursuit (OMP) algorithm [6] which modifies MP such that the orthogonal projection is performed after each iteration: Once a new vector is added to the set of selected vectors \mathbf{S} , the coefficients \mathbf{c} are computed by an orthogonal projection of \mathbf{y} onto \mathbf{S} . This modification ensures orthogonality of the residue to the set \mathbf{S} after each iteration and enhances the reconstruction accuracy.

A detailed analysis of OMP is provided in [22] which states a lower-bound on the number of observations for exact recovery. Let the observation matrix be composed of M i.i.d. measurement vectors from the Gaussian distribution. Then, for a fixed $\delta \in (0, 0.36)$, each K -sparse signal can be reconstructed via OMP with probability exceeding $1 - 2\delta$ where the number of measurements should be chosen according to $M \geq \beta K \ln N / \delta$ where β is a parameter. Choosing $\beta \approx 20$ is necessary for theoretical results, while it is enough to set $\beta \approx 4$ when K is large. The guarantees for OMP, however, were shown to be non-uniform, i.e. they hold only for each fixed sparse signal, but not for all [7]. It was shown in [23] that for natural random matrices it is not possible to obtain uniform guarantees for OMP.

4.3. Subspace Pursuit

A recent proposal, Subspace Pursuit (SP) [8], is based on a search of the sparse representation in a subspace of the initial basis, which is modified at each iteration. Each iteration starts with an initial representation (support) having K vectors, which is first enlarged by adding the best K vectors among the unused ones in the basis. The measured signal is then projected orthogonally onto this subspace of $2K$ vectors, after which the subspace is pruned to contain the best K candidates.

A very similar approach is the Compressive Sampling Matching Pursuit (CoSaMP) [9], where the main difference to SP is the number of vectors added to the support at the beginning of each iteration. CoSaMP enlarges the support by adding $2K$ components instead of K as for SP.

As a result of decreasing the number of components which are added to the support at each iteration, SP is computationally less expensive than CoSaMP. Another consequence of it is that RIP condition necessary for exact reconstruction becomes less restrictive. For exact reconstruction using CoSaMP, the observation matrix should obey RIP with $\delta_{4K} \leq 0.1$ or equivalently $\delta_{2K} \leq 0.025$ as stated in [9]. SP, on the other hand, necessitates a weaker condition, $\delta_{3K} \leq 0.165$ [8].

5. A* Search

Before going on with our proposal, we find it beneficial to devote this section to a short discussion about the A* Search technique [10, 11, 12, 13, 14]. Below, we introduce A* search for a minimization problem. We also mention some modifications of the algorithm in order to make it more appropriate for our purposes.

5.1. Fundamentals of A* Search

A* search is an iterative tree-search algorithm for finding the complete path that fulfills some criterion, which in our case corresponds to minimizing an evaluation function. Paths of the A* search tree are built up by nodes that are elements of a finite set representing the search space. In this discussion, a *complete* path refers to a path that has desired number of nodes, and a shorter path is called *partial*. A* search starts with an initial tree consisting of only partial paths. Each

iteration selects the most promising path on the tree, i.e. the path that is expected to minimize the evaluation function, and the search tree is expanded by adding one or more nodes to this path. Iterations are repeated until a complete path is selected as the most promising path.

For CS reconstruction purposes, nodes represent the basis vectors and the goal of the search is to find the complete path of length K to represent K -sparse signal. To illustrate, let p^i denote the i 'th node on the complete path $\mathbf{p}^K = p^1, p^2, \dots, p^K$ and $g(\mathbf{p}^K)$ be the evaluation function for \mathbf{p}^K . We are interested in finding the complete path $\hat{\mathbf{p}}^K$ that leads to the minimum value of the evaluation function

$$\hat{\mathbf{p}}^K = \arg \min_{\mathbf{p}^K} g(\mathbf{p}^K). \quad (16)$$

where $g(\mathbf{p}^K)$ depends on all K nodes p^i , $i = 1, 2, \dots, K$ on the path.

As a consequence of its nature, each A* iteration has to find the most promising path on a tree which consists of partial paths with different lengths and maybe some complete paths. This is not trivial for such an incomplete tree: First, we cannot compute the evaluation function $g(\mathbf{p}^K)$ exactly for partial paths because of lacking nodes. Second, even if it is possible to compute a partial evaluation function $g(\mathbf{p}^l)$ using the $l < K$ identified nodes on a partial path, different path lengths still make the comparison nonsense.

In order to deal with different path lengths, A* search utilizes a compensation mechanism that employs an auxiliary function [12]. For a partial path of length $l < K$, the auxiliary function $d(\mathbf{p}^l)$ can be defined such that $d(\mathbf{p}^K) = 0$ and

$$d(\mathbf{p}^l) \geq g(\mathbf{p}^l) - g(\mathbf{p}^l \cup \mathbf{z}^{K-l}), \quad \forall \mathbf{z}^{K-l}, \quad (17)$$

where \mathbf{z}^{K-l} is a sequence of $K - l$ nodes and $\mathbf{p}^l \cup \mathbf{z}^{K-l}$ is the concatenation of \mathbf{p}^l and \mathbf{z}^{K-l} , leading to a complete path. With this definition, the auxiliary function $d(\mathbf{p}^l)$ is larger than or equal to the decrement in the evaluation function that any complete extension of the path \mathbf{p}^l would yield.

Now, we can define the cost function

$$F(\mathbf{p}^l) = g(\mathbf{p}^l) - d(\mathbf{p}^l). \quad (18)$$

Let's consider a complete path \mathbf{p}^K and a partial path $\tilde{\mathbf{p}}^l$ of length $l < K$. Combining (17) and (18), we can conclude that if $F(\mathbf{p}^K) \leq F(\tilde{\mathbf{p}}^l)$, then $g(\mathbf{p}^K) \leq g(\tilde{\mathbf{p}}^l \cup \mathbf{z}^{K-l})$ for all \mathbf{z}^{K-l} . Hence, no extension of path $\tilde{\mathbf{p}}^l$ may lead to a lower evaluation function value than that of the path \mathbf{p}^K , and $\tilde{\mathbf{p}}^l$ can be safely removed from the search [12]. Therefore, selecting the most promising partial path can be performed via the cost function $F(\mathbf{p}^l)$. Note that, in practice it may not be possible to find an auxiliary function that exactly satisfies (17) or it may not be beneficial to use such an auxiliary function for search efficiency. This issue will be discussed when different A*OMP cost models are introduced in Section 6.3.

Finally, we can outline a standard A* search as follows: It starts with an initial tree of all possible single-node paths. At each iteration, the cost function $F(\cdot)$ is computed for all paths and the path with the minimum cost is chosen. All possible extensions of this path (by adding a single node for each) are added to the tree. In this manner, the tree is expanded until the search finds a complete path that has minimum cost. This path is taken as the final decision.

5.2. Different Auxiliary Cost Function Structures

The auxiliary function plays an important role in the final performance of the A* search algorithm, as any non-suitable auxiliary function would result in selecting non-optimal paths and

failure of the search. The reasonable selection of the auxiliary function is trying to mimic the decay of the cost function over path length. For this purpose, it is beneficial to consider different structures for the auxiliary function, which exploit different assumptions about the decay in the cost.

The typical choice for the structure of the auxiliary function in (18) employs an additive model following [12]. Based on this structure, it is possible to determine the value of the auxiliary function in different ways. In Section 6.3, we derive two different cost models from this structure. For the first one, which we call additive cost model, we assume that each node is expected to decrease the cost by a constant value, i.e. the value of the auxiliary function becomes a constant value times the number of unassigned nodes in a partial path. In contrast to this static model, we also propose an adaptive cost model, where the expected decrease in cost per node is determined adaptively by the decrease in cost occurred during the addition of the previous node to a partial path. In fact, simulation results given in Section 7 state that this adaptive model improves the performance of A* search in the sparse signal reconstruction problem.

Addition is only one possible (in fact, commonly used) structure for the auxiliary function. Auxiliary function may be structured in various forms depending on the structure of the problem. For our purposes, we propose a structure which employs a multiplicative auxiliary function model. This model is called the multiplicative cost model, which is based on the assumption that each node reduces the cost by some constant ratio:

$$F_{mul}(\mathbf{p}^l) = \alpha^{K-l} g(\mathbf{p}^l), \quad (19)$$

where $0 < \alpha < 1$.

These two structures will form the basis for the cost models we develop for A*OMP. As these make much sense in the context of A*OMP, a detailed discussion of these structures will be covered in Section 6.3, in combination with the path selection mechanism of A*OMP.

6. Sparse Signal Reconstruction using A* Search

RIP appears as an important means for theoretical guarantee of sparse signal representation algorithms. In the previous section, we mentioned that when RIP is satisfied for some constants, algorithms such as BP, SP, ROMP, CoSaMP etc. can provide exact reconstruction. Though not uniform, there are also some guarantees for OMP. Satisfying RIP requirements for real problems, however, may sometimes be a problem. Although some random matrices, such as the ones drawn from i.i.d. Gaussian or Bernoulli distributions, are shown to satisfy RIP with high probabilities when certain conditions are satisfied, the number of random observations required for satisfying RIP with high probabilities increases with the sparsity number K . In other words, if the number of observations is kept constant, the probability of exact reconstruction decreases with increasing K . Incorporation of a multi-path search strategy is motivated by the expectation that such an algorithm improves reconstruction at sparsity levels especially where the exact reconstruction probability of a single-path algorithm (or BP) starts falling.

The semi-greedy multi-path search strategy proposed in this work is referred to as A* Orthogonal Matching Pursuit (A*OMP). A*OMP algorithm casts the problem of finding the correct set of vectors for representing the signal into searching for the best set of vectors among a number of candidate sets. For this purpose, a number of candidate representations are obtained in an iterative manner, employing A* Search. That is, we start with an initial set of representations, or

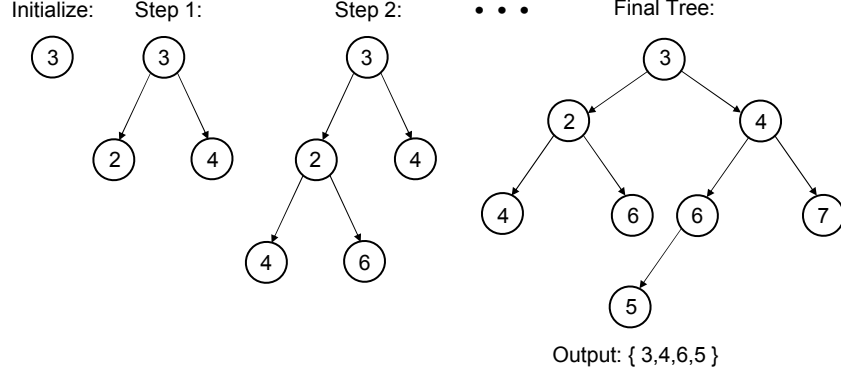


Figure 1: Evaluation of the search tree during A*OMP algorithm

so called paths, and at each step, new basis vectors are added to the most promising path, which is found utilizing some cost function based on the instantaneous reconstruction error. In other words, this method is based on performing a multi-path search for the best K -sparse representation of the vector \mathbf{y} among all possible representations which the N elements of the holographic basis \mathbf{V} may provide. In a tree-based representation, we can model these representations as complete paths with K nodes, each of which correspond to a vector in the basis \mathbf{V} . The search for the required representation among the set of all possible representations, the search space, can now be performed on a search tree employing the A* search algorithm. The evaluation of such a search tree throughout the search process is illustrated in Fig. 1.

As this approach does not rely only on a single set, but a number of candidates, which are computed simultaneously, we expect it to reduce the amount of reconstruction error by getting rid of many errors into which a single path would fall because of the linear dependency of basis vectors. That is, even if computation of a single path would yield a wrong representation in some cases, the correct one will mostly be in the set of candidate representations. Hence, we claim that the requirement of satisfying RIP can be relaxed, at least around sparsity levels where exact reconstruction probability falls, and the proposed approach provides high reconstruction rates. This claim, of course, should not mislead the reader to the wrong idea that we do not need RIP at all. In contrast, we acknowledge the RIP as a natural condition following the linear dependency of holographic basis vectors, and look for a greedy way which does not aim to directly obtain a weaker RIP requirement, but tries to improve the reconstruction in situations where RIP may not be satisfied for a single-path search.

For the rest of this work, we differentiate between the paths in the search stack with subscripts. When necessary, the notation introduced in Section 4.1 is extended such that the defined variables include subscripts that represent which path the variable belongs to. The superscripts, as before, represent the length of the path, or the position of the node in the path to which the variable belongs. \mathbf{s}_i^l represents the selected basis vector at node l on path i and c_i^l the corresponding coefficient. Similarly \mathbf{r}_i is the residue of path i . \mathbf{S}_i and \mathbf{c}_i denote the matrix of vectors selected for path i and the vector of corresponding coefficients respectively. Note that \mathbf{S}_i and \mathbf{s}_i^l are in fact the mathematical equivalents of the corresponding path and node, respectively. Below we slightly abuse this notation for simplicity and use \mathbf{s}_i^l and \mathbf{S}_i also to represent the corresponding node and path.

Having stated how the problem is casted into a tree-based representation, utilization of tree search can now be discussed. For this purpose, three main steps of the search, initialization of the search stack, selecting the best path among the stack and expansion of the selected partial path are explained below. Finally we present an overview of the whole algorithm.

6.1. Initialization of the Search Stack

As discussed above, A* search incorporates all single node paths by adding them to the initial search stack. In our problem, this corresponds to initializing the search stack with N representations, each having a single particular vector from the holographic basis. This approach would, of course, be complete as all possible single node paths are included in the search, however it will not be practical in most cases as N might be large. In fact, most of the vectors in the holographic basis are irrelevant to the signal \mathbf{y} , and the corresponding paths in the initial stack will not be chosen for expansion if the evaluation criterion is selected appropriately. Clearly, the number of meaningful initial paths is K . Though these K paths are obviously not known a priori, this fact makes it safe to restrict the initial stack only to about K vectors that best match \mathbf{y} .

In addition, we also incorporate the structure of the reconstruction problem to further reduce the number of initial paths. In the CS reconstruction problem, the order in which the basis vectors are added to the representation throughout the search is not important. As the algorithm takes into account more than one extensions of a selected partial path, (Section 6.2) even when all possible initial paths are not included in the search, we can claim the algorithm will have a strong reconstruction ability.

As a result of this discussion, the initial search stack will be kept limited to the $I \ll K$ vectors that have the highest absolute inner-product with \mathbf{y} . Another approach would be incorporating a dynamical initial search stack size, by adding the vectors whose inner-product with the vector \mathbf{y} is larger than a certain threshold to the initial stack. However we will follow the first suggestion in this work, and the results provided in Section 7 indicate that this choice is indeed able to improve reconstruction performance.

6.2. Expanding the Selected Partial Path

We now focus on the problem of expanding the selected partial path. In typical A* search, all possible extensions of the selected partial path are added to the stack at each iteration. Similar to the initialization step, this approach may result in very large search stacks in real problems because of the high number of possible extensions. To illustrate, let the length of the selected partial path be l . Then the number of possible extensions, which can be obtained by adding one vector to this path, is $N - l$. As we deal with sparse vectors, l is usually much smaller than N , hence the algorithm requires approximately N paths to be added to the stack at each iteration. Therefore, in case of a full A*-search, the number of search paths kept in the stack may finally increase up to N^K , given $K \ll N$.

In order to overcome the problem of too many search paths, we suggest three pruning strategies, depending on number of extensions per path, maximum allowable search stack size and path equivalency. Below, we discuss these strategies in detail.

6.2.1. Extensions per Path Pruning

This strategy proposes to consider not all possible extensions but only the most promising ones. Similar to the initialization step, only a small number candidates which yield the highest inner-product values with the residue of the partial path are added to the stack at each iteration.

As above, we make use of the unimportance of the order of selected vectors, noting that at each step we only need to add one of the K vectors to the representation, and not a specific one of them. In other words, permutations of selected vectors within the representation do constitute equivalent paths, and are not important for our purpose. Therefore, considering only a few candidates per selected partial path becomes a reasonable choice to reduce the number of candidate paths in the stack. Following this discussion, at each iteration of the search, we consider only B of the all possible branches that might emerge from the selected partial path. As for initialization, the number of branches might be kept dynamic, such that extension is performed only if the new node has high correlation with the residue, however we prefer a fixed number of branches in this work.

To restrict the number of branches added to the stack per selected partial path, inner products of the basis vectors with the residue of the path is considered and the ones with higher inner products are chosen, as mentioned above. Following this, the residue for the new path should be computed. In Section 4.2, it was already mentioned, however, that choosing the inner-product value as the coefficient of the selected vector is not optimal for representing \mathbf{y} , as the vectors in the holographic basis \mathbf{V} are not orthogonal to each other. Hence, as for OMP, the optimal coefficients and residue for the new path are obtained by orthogonal projection of \mathbf{y} onto the set of basis vectors selected by the path. The orthogonalization of the residue is an extremely important step for the search, as extensions of the path are selected wrt. this residue.

In case of a full A* search, the maximum number of paths in the stack is upper-bounded by N^K , as indicated above. By restricting the number of branches per partial path, the bound is decreased to B^K . When the number of initial paths is selected as I , the maximum number of paths in the search stack are limited by $I * B^{(K-1)}$. Ideally, I and B are chosen much smaller than K , hence these choices reduce the number of candidates in the search path drastically.

6.2.2. Stack Size Pruning

Though we have decreased the maximum number of search paths, we can still ask the following question about the size of the search stack: Is it really necessary to keep all the paths in the search stack till the search ends or can we remove some of them when new paths are inserted? A* search adds new paths to the stack at each iteration and the number of these can still go very high for many applications, because of not only the required computational complexity, but also the memory needs, as the corresponding residues are also necessary. The strategy which we apply in this work to deal with this problem is to limit the number of paths in the stack by P , such that when this limit is exceeded, a new path replaces the worst path, i.e. the path with maximum cost in the stack, only if its associated cost is smaller than that of the worst path, and otherwise neglected. This strategy is known as “beam search” as well.

Fig. 2 illustrates the Extensions per Path and Stack Size Pruning rules. Evaluation of the search tree during a single iteration of the A*OMP algorithm is depicted. Initial state of the tree is given in Fig. 2a. In this example we set $P = 4$ and $B = 3$, i.e. 4 paths are allowed in the stack and each selected partial path is extended by three branches. Each leaf of the tree corresponds to a different path and there are paths with different lengths. The cost of each path, C_i , whose computation is mentioned below, is indicated near the corresponding leaf. We would like to extend the best path, i.e. the one with minimum cost, which is Path 4 in our case. First, we find the B basis vectors that yield the highest inner-product with the residue. For this illustration, let the nodes corresponding to these vectors be the '2', '8' and '9', ordered with decreasing inner-product values. Obviously, the first extension of the best path can safely replace the best path itself. Fig. 2b shows the tree after the first extension of Path 4 obtained by concatenation of the node '2' directly replaces Path

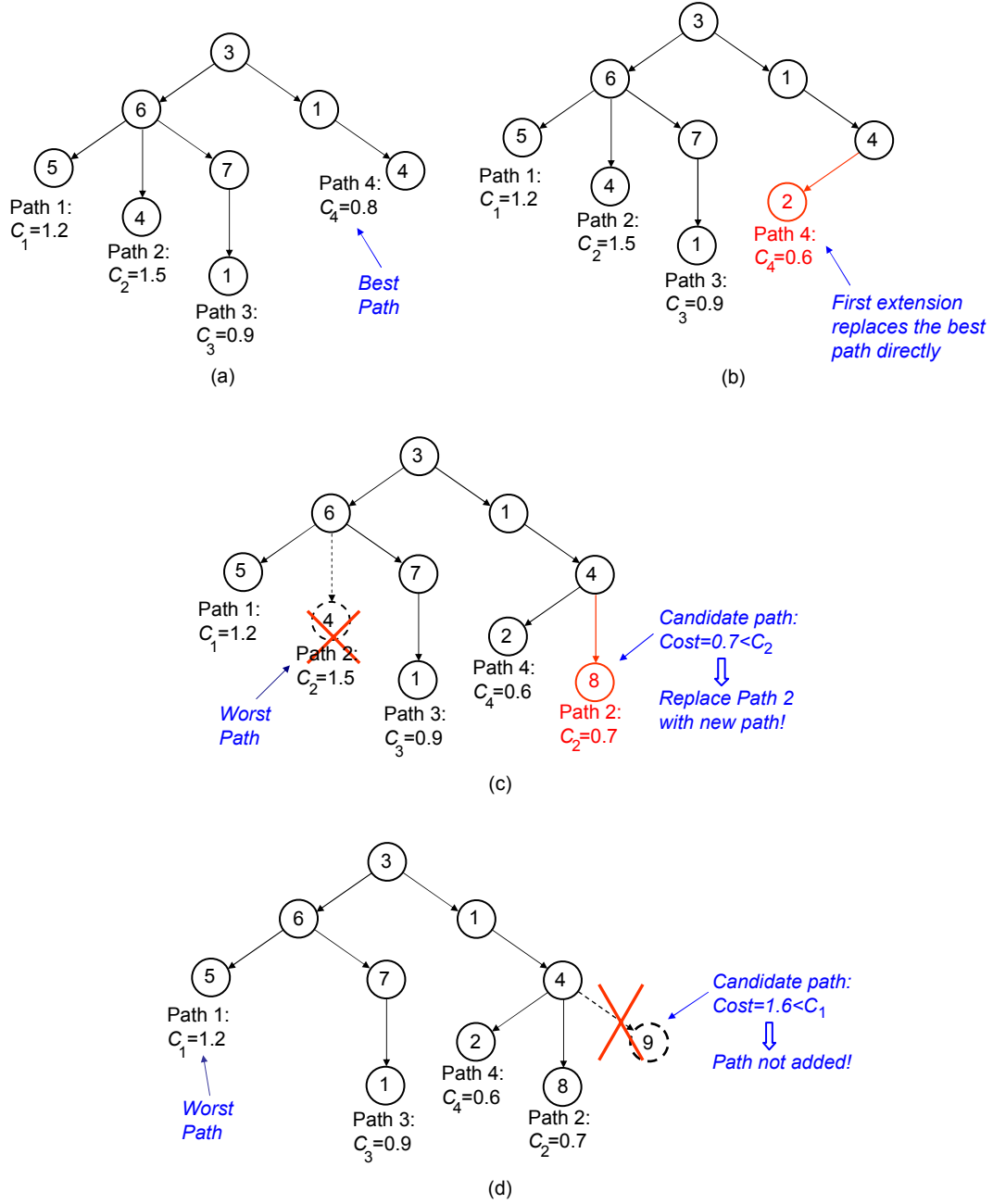


Figure 2: Evaluation of the search tree during a single iteration of the A*OMP algorithm

4. Extension with the node '8', which is the second best node, yields the second candidate path as depicted in Fig. 2c. The cost of this candidate path is 0.7. As there are already 4 paths in the stack, and the number of maximum paths is limited to $P = 4$, we need to find the worst path in the tree and compare its cost with this candidate path. As illustrated, Path 2 is the worst path with the maximum cost, and its cost is higher than the candidate path. Hence, Path 2 is removed from the stack by deletion of the corresponding leaf and the candidate path is added into the tree

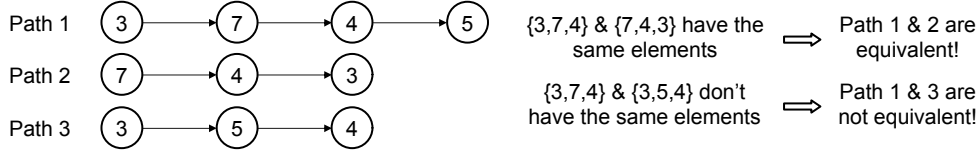


Figure 3: Path Equivalency: Path 1 and Path 2 are equivalent as first three nodes of Path 1 contain only nodes in Path 2. Path 3 is not equivalent to Path 1 as node 5 is not an element of the first three nodes of Path 1. Note that orthogonal projections ensure Path 2 to select node 5 as the next node, while there is no guarantee that Path 3 will select node 7.

by adding the leaf '8' as shown. Finally, the third extension is to be considered by using node '0'. As given in Fig. 2d, the cost of this candidate path is higher than the cost of the worst path, which is now Path 1. Hence, this candidate path is not added to the search tree. This completes the extension of Path '4' and ends one iteration of the algorithm.

6.2.3. Equivalent Path Pruning

A final point that can improve the performance and reduce the growth of the search stack is avoiding equivalent paths in the stack. This strategy is explained by the following rule: When a new path is to be inserted into the stack, we check if this path has already been considered at previous iterations of the search. A new path is to be inserted into the stack only if it was not considered at previous stages. Application of this rule, however, is tricky, because the condition for equivalence of two paths is not obvious, especially when they have different lengths. As permutations of vectors within the sparse representation does not matter, it is not enough to simply compare the paths. For equivalency of two paths, we define the following notion: Let $S_1^{l_1}$ and $S_2^{l_2}$ be two paths of lengths l_1 and l_2 , respectively, where $l_1 \geq l_2$. Let's define $S_{p,1}^{l_2}$ as the partial path that contains only the first l_2 nodes of $S_1^{l_1}$, i.e. $S_{p,1}^{l_2} = s_1^1, s_1^2, \dots, s_1^{l_2}$. We say $S_1^{l_1}$ and $S_2^{l_2}$ are equivalent if and only if $S_{p,1}^{l_2}$ and $S_2^{l_2}$ share the same set of nodes. Then, the orthogonalization of the residue at each expansion ensures that the residue of $S_2^{l_2}$ is equal to the residue of $S_{p,1}^{l_2}$ and expansions of $S_{p,1}^{l_2}$ and $S_2^{l_2}$ will yield the same paths. As $S_1^{l_1}$ already exists in the stack, we know that $S_{p,1}^{l_2}$ has already been expanded in previous iterations and addition of $S_2^{l_2}$ into the stack is unnecessary.

This notion of path equivalency is illustrated in Fig. 3. Path 2 contains the nodes 7,4,3. We observe that the first three nodes of Path 1 do also employ the same set of nodes, making Path 1 and Path 2 equivalent. Equivalency of these is ensured by the orthogonalization step, which guarantees Path 2 to select node 5 as the next node. As a result of equivalency notion, Path 2 might be safely removed from the search tree. On the contrary, Path 1 and Path 3 are not equivalent as the first three nodes of Path 1 do not contain the same nodes as in Path 3. Though the set of nodes in Path 3 is a subset of all nodes in Path 1, there is no guarantee that Path 3 will be extended by node 7 next. Hence they represent different hypotheses spaces.

6.3. Selection of the Best Path

Last point to be clarified before applying the tree-search on the reconstruction problem is how to select the best path in the search stack at each iteration. A natural evaluation criterion for the best path is the minimum ℓ_2 norm of the approximation error (residual norm), as we are finally interested in the representation with the smallest error. Then, for a path \mathbf{S}^l of length l , the

evaluation function becomes

$$g(\mathbf{S}^l) = \left\| \mathbf{y} - \sum_{j=1}^l c^j \mathbf{s}^j \right\|_2, \quad (20)$$

where \mathbf{s}^j and c^j denote the selected basis vector at stage j and the corresponding coefficient respectively.

As paths with different lengths cannot be directly compared to each other during the search, it is essential to define an auxiliary function in order to compensate for different path lengths. This choice should be done carefully, because any non-suitable auxiliary function would result in selecting non-optimal paths and failure of the search. Ideally, one would mimic the ideal behavior of the decay in the residue, however it is obviously not possible to observe this value directly. In this work, we will consider three different methods which exploit different assumptions about the decay in the residue at each node on a path.

6.3.1. Additive Cost Model

For the first, we assume that each of the K vectors in the representation make equal contributions to $\|\mathbf{y}\|_2$. That is, let the addition of a correct vector to the representation decrease the error norm on average by

$$\delta_e = \frac{(\|\mathbf{y}\|_2)}{K}. \quad (21)$$

Following this, addition of remaining $K - l$ nodes to a path of length l is expected to decrease the error norm by an amount of $(K - l)\delta_e$. From the discussion in Section 5, we conclude that the auxiliary function should satisfy

$$\begin{aligned} d_{add}(\mathbf{S}^l) &\geq (K - l) \delta_e \\ &\geq (K - l) \frac{\|\mathbf{y}\|_2}{K}. \end{aligned} \quad (22)$$

Regarding this discussion, we choose the auxiliary function as

$$d_{add}(\mathbf{S}^l) = \beta(K - l) \frac{\|\mathbf{y}\|_2}{K}, \quad (23)$$

where β is a constant greater than 1. Finally we can write the objective function $F(\mathbf{S}^l)$, as

$$F_{add}(\mathbf{S}^l) = \left\| \mathbf{r}^l \right\|_2 - \beta \frac{(K - l)}{K} \|\mathbf{y}\|_2. \quad (24)$$

We will refer to this objective function from now on as the additive cost function. The term cost function suits our purposes better as we are interested in minimizing it.

The assumption that each vector individually makes equal contribution to $\|\mathbf{y}\|_2$ obviously may not hold in general. However, as this assumption is valid on average, the auxiliary function in (22) is still larger than the expected decrease of the error norm in the remaining $K - l$ nodes. Moreover, one would intuitively expect the search to make more mistakes at vectors with smaller contributions to $\|\mathbf{y}\|_2$, and for these, the auxiliary function will satisfy the requirement with much higher probability. The parameter β , here, plays a role similar to a regularization constant. If β is large, shorter paths are favored against longer ones while choosing the best path, making the search expand more candidates. When it becomes smaller, longer paths will have a higher chance to be expanded.

6.3.2. Adaptive Cost Model

In contrast to the equal contribution assumption above, the auxiliary function can also be chosen in a dynamic manner, based on the previous decrease of the residue for each path in stack. That is, for each path, the decrease in the ℓ_2 norm of the residue for the last node of the path is utilized for computing the auxiliary function. As the selection of vectors throughout the search is based on their correlations with the residue, the algorithm is expected to select first the vectors whose contributions to the signal \mathbf{y} are large. Hence, the decrease in the residue wrt. selecting a vector at a stage will generally be larger than the decrease that will occur in a later iteration. This information can be used by modifying the expected change in the error norm in (21) as:

$$\delta_e = \left(\left\| \mathbf{r}_i^{l-1} \right\|_2 - \left\| \mathbf{r}_i^l \right\|_2 \right). \quad (25)$$

Then, similar to the additive auxiliary function above, we conclude that the new adaptive auxiliary function should satisfy

$$d_{adap}(\mathbf{S}_i^l) \geq (K-l) \left(\left\| \mathbf{r}_i^{l-1} \right\|_2 - \left\| \mathbf{r}_i^l \right\|_2 \right), \quad (26)$$

where the subscript i denotes the dependency of the auxiliary function on the path i . As for the additive case, we incorporate the parameter β to finally obtain the auxiliary function

$$d_{adap}(\mathbf{S}_i^l) = \beta \left(\left\| \mathbf{r}_i^{l-1} \right\|_2 - \left\| \mathbf{r}_i^l \right\|_2 \right) (K-l), \quad (27)$$

where $\beta > 1$ as above. The adaptive cost function can then be written as follows:

$$F_{adap}(\mathbf{S}_i^l) = \left\| \mathbf{r}_i^l \right\|_2 - \beta \left(\left\| \mathbf{r}_i^{l-1} \right\|_2 - \left\| \mathbf{r}_i^l \right\|_2 \right) (K-l). \quad (28)$$

6.3.3. Multiplicative Cost Model

Above, we discussed auxiliary functions which are added to (or subtracted from) the cost, following the definition of A* search [12]. In contrast to addition of the auxiliary function, multiplication of the evaluation function with a weighting function also provides means for compensation of path length differences. In this approach, we assume that addition of one vector to the representation reduces the residual error by a constant ratio, α . That is, we define the cost function of a path of length l as

$$F_{mul}(\mathbf{S}_i^l) = \alpha^{K-l} g(\mathbf{S}_i^l) = \alpha^{K-l} \left\| \mathbf{r}_i^l \right\|_2. \quad (29)$$

This cost function will be referred to as the multiplicative cost function. For the cost function to be meaningful, α should be chosen between 0 and 1. The value of α defines how fast the cost function will decay. When α gets close to 0, cost of expanding shorter paths becomes very small, letting the search to expand them. On the contrary, if α is chosen to be close to 1, weighting will hardly change the value of the cost function, hence longer paths will be favored. Therefore, the role of α is very close to that of β for the additive cost function.

We would like also to note that an adaptive version of the multiplicative cost function is also possible with an appropriate strategy that adjusts the ratio of the expected decay in the residue during the search process. This strategy is not discussed in this manuscript, however it is considered as one of the future directions.

Comparison of these three different cost functions leads to the fact that they make different assumptions about the decay of the error. The additive one is based on the assumption that error is

expected to decrease in equal amounts at each iteration. On the other hand, in case of the other two dynamic cost functions, the expected decay in the residue is modified wrt. the actual knowledge about the path. Also, multiplicative cost function always yields a positive cost, while the additive ones can also be negative. Hence, these cost functions are expected to provide a better modeling of the decrease in the residue norm or at least provide a closer bound, and improve the search. The improvement here is not only in terms of reconstruction rates, but also in terms of search time as these dynamic cost functions yield a far more effective solution for compensating between different path lengths, increasing the accuracy of the candidate selection process and allowing the A* search to find the solution in less number of iterations. The simulation results provided in Section 7 clearly indicate the effectiveness of a dynamic cost model.

6.4. A* Orthogonal Matching Pursuit

After having discussed the fundamental problems, we can finally present the A*OMP algorithm in its complete form. The procedure can be outlined as follows: First, we initialize I out of P paths such that each include one of the I vectors which best match \mathbf{y} and the remaining $P - I$ paths are left empty. The cost for these empty paths is the ℓ_2 norm of \mathbf{y} , hence they are the worst paths in the search stack and will be removed first. After search stack is initialized, the most promising path in the stack is selected wrt. the chosen cost function and expanded. During expansion, B new paths are obtained from the selected path as discussed in Section 6.2. Unless these new paths are not equivalent to the ones in the search stack, best of them replaces the selected path, while others replace the worst paths in the stack if their cost is lower than these. The residues of these recently added paths and the optimal coefficients are obtained by orthogonal projection of the signal \mathbf{y} onto the set of vectors in each path. The process of selecting and expanding the most promising path is iterated until the selected path has length K . The pseudo-code for the algorithm is given in Algorithm 1.

Though this work is limited to signals of known sparsity number, K , the authors would like to note that it is possible to change the convergence criterion of the A*OMP in order to reconstruct signals whose sparsity numbers are not known a priori. A number of different criteria might be incorporated for this purpose, for example, norm of the residue falling below a threshold, or no further reduction of the residue obtained by further iterations.

With the given structure, A*OMP can be seen as a multi-path OMP algorithm where the paths are chosen in an intelligent manner by utilizing an auxiliary cost function. Selection of an appropriate auxiliary cost function, for which some examples are provided in Section 6.3, makes the search process more effective. By an appropriate evaluation of these multi-paths, though any single one of these are limited to the RIP condition of OMP algorithm alone, A*OMP can relax the RIP condition, increasing the probability of finding a final path that is not altered by the linear dependency of the vectors in the holographic basis \mathbf{V} .

6.5. Complexity vs. Accuracy

A final point to note before closing this section is the relation between complexity and accuracy of the A*OMP. The pruning strategies which are listed above can be seen as a trade-off between the accuracy and complexity of the algorithm. Letting the pruning parameters be as large as possible, that is $I = N$, $B = N$ and $P = \infty$, the algorithm will perform an exhaustive search, trying to evaluate all possible representations. On the other hand, setting $I = 1$ and $B = 1$ results in an OMP search (Note that P becomes nonsense in this case, as there is only a single path.). Exhaustive search is obviously prohibitively complex in most situations, while the simple OMP

Algorithm 1 A* ORTHOGONAL MATCHING PURSUIT

Define:

$P :=$ Maximum number of search paths, $I :=$ Number of initial search paths

$B :=$ Number of extended branches per iteration

$\mathbf{S}_i = \{\mathbf{s}_i^l\}$, matrix of vectors \mathbf{s}_i^l selected at the i 'th path

$\mathbf{c}_i = \{c_i^l\}$, vector of coefficients for the selected vectors on the i 'th path

$L_i :=$ length of the i 'th path, $C_i :=$ cost for selecting the i 'th path

Initialize:

$\mathbf{T} \leftarrow \emptyset$

for $i \leftarrow 1$ to I **do**

$\triangleright I$ paths of length 1

$\hat{n} \leftarrow \arg \max_{n, \mathbf{v}_n \in \mathbf{V} \setminus \mathbf{T}} \langle \mathbf{y}, \mathbf{v}_n \rangle$

$\mathbf{T} \leftarrow \mathbf{T} \cup \mathbf{v}_{\hat{n}}, \mathbf{s}_i^1 \leftarrow \mathbf{v}_{\hat{n}}, c_i^1 \leftarrow \langle \mathbf{y}, \mathbf{v}_{\hat{n}} \rangle$

$\mathbf{r}_i \leftarrow \mathbf{y} - c_i^1 \mathbf{s}_i^1, C_i = F(\mathbf{S}_i), L_i = 1$

end for

$C_i = \|\mathbf{y}\|_2, L_i = 0, \forall i = I + 1, I + 2, \dots, P$

$best_path \leftarrow 1$

while $L_{best_path} \neq K$ **do**

$\hat{p} \leftarrow best_path, \mathbf{T} \leftarrow \mathbf{S}_{best_path}$

\triangleright best path is replaced by its first extension

for $i \leftarrow 1$ to B **do**

$\hat{n} \leftarrow \arg \max_{n, \mathbf{v}_n \in \mathbf{V} \setminus \mathbf{T}} \langle \mathbf{r}_{best_path}, \mathbf{v}_n \rangle$

$\mathbf{T} \leftarrow \mathbf{T} \cup \mathbf{v}_{\hat{n}}$

$\hat{\mathbf{S}} \leftarrow \mathbf{S}_{best_path} \cup \mathbf{v}_{\hat{n}}$

\triangleright Candidate path

if $(F(\hat{\mathbf{S}}) < F(\mathbf{S}_{\hat{p}})) \ \& \ (\hat{\mathbf{S}} \neq \mathbf{S}_j, \forall j = 1, 2, \dots, P)$ **then**

\triangleright if candidate path is better than

worst and is not already in search tree

$\mathbf{S}_{\hat{p}} \leftarrow \hat{\mathbf{S}}, L_{\hat{p}} \leftarrow L_{best_path} + 1, \mathbf{c}_{\hat{p}} \leftarrow \arg \min_{\alpha} \|\mathbf{y} - \hat{\mathbf{S}}\alpha\|_2$

$\mathbf{r}_{\hat{p}} \leftarrow \mathbf{y} - \mathbf{S}_{\hat{p}}\mathbf{c}_{\hat{p}}, C_{\hat{p}} \leftarrow F(\hat{\mathbf{S}})$

\triangleright update \hat{p}

end if

$\hat{p} \leftarrow \arg \max_{i \in \{1, 2, \dots, P\}} C_i$

\triangleright select worst path to be replaced by next extension

end for

$best_path \leftarrow \arg \min_{i \in \{1, 2, \dots, P\}} C_i$

\triangleright select best path

end while

return $\mathbf{S}_{best_path}, \mathbf{c}_{best_path}$

mostly lacks high reconstruction accuracy. However, the pruning parameters of A*OMP provide means for a choice between the complexity of the search and accuracy of the solution.

The choice for the auxiliary cost function is also extremely important in this trade-off, as an appropriate modeling of the decay of the residue along nodes provides the algorithm the ability to distinguish between branches which the solution might lie and on which might not. In other words, the choice of the auxiliary cost function is important for the pruning to be effective. With an appropriately chosen auxiliary function, the trade-off between the complexity and accuracy might be boosted in favor of accuracy.

7. Simulation Results

In order to demonstrate the reconstruction capability of the proposed A*OMP algorithm, we consider two series of simulations in which we compare A*OMP to BP, SP and OMP. In addition, performance of variants of A*OMP, which incorporate different cost functions and number of branches, are also compared. First series of these simulations were performed using a synthetically generated 1D data set and different bases. The latter, on the other hand, demonstrates the performance of the mentioned algorithms in a real image reconstruction problem, which involves some commonly used test images.

7.1. Reconstruction of Synthetically Generated 1D Data

The first set of simulations consists of evaluation of the algorithm over different orthogonal bases. Among various possible orthogonal bases, the DCT and Haar Wavelet bases were employed as these are among the most commonly used ones in signal processing and compression. In these cases, the vectors are themselves not sparse, but have sparse representations in terms of the basis vectors. In addition to these, simulations were also performed using vectors that are sparse themselves. This case can be seen as a Dirac Basis, where the basis vectors consist of delayed Dirac's i.e. the i 'th basis vector is $\psi_i = \delta[n - i]$, $i = 0, \dots, N - 1$. Each of these bases have 256 dimensions, i.e. the vectors which should be reconstructed are of length $N = 256$.

For each test, 500 test vectors were randomly drawn from basis vectors of each basis. Each test vector is composed of K random components selected among the 256 equally probable basis vectors, where the coefficients of selected vectors were also drawn randomly. In order to compare performance, the simulations were repeated for different coefficient distributions. These include coefficients drawn from uniform and normal distributions as well as binary coefficients, where all non-zero coefficients were set to 1.

From each test sample, $M = 100$ random observations were taken. That is, the problem is reconstructing each vector of length $N = 256$ from its random observation of length $M = 100$. A different observation matrix Φ was employed for each of the vectors in order to generalize the performance. Entries of the observation matrices were modeled as iid Gaussian random variables with mean 0 and standard deviation $1/N$.

Three versions of the A*OMP approach were evaluated in comparison to BP, SP and OMP algorithms. These incorporate additive, adaptive and multiplicative cost models and hence are abbreviated as Add-A*OMP, Adap-A*OMP and Mul-A*OMP, respectively in the rest of this manuscript. For all tests, search stack was initialized to involve $I = 3$ non-empty paths and at each iteration, $B = 2$ branches are added to the search tree. The number of maximum paths, P , was chosen as 200. The parameters of the auxiliary functions were selected as $\beta = 1.25$ and $\alpha = 0.5$. The algorithms were run for 500 generated samples to generalize performance. Reconstruction accuracy was obtained in terms of both the average normalized mean squared error ($NMSE$) over 500 samples and exact reconstruction rate. For the vector \mathbf{x} , $NMSE$ was computed as

$$NMSE = \frac{\|\mathbf{x} - \hat{\mathbf{x}}\|_2}{\|\mathbf{x}\|_2} \quad (30)$$

and final average NMSE was obtained as an average over 500 samples. Similarly, exact reconstruction rate provides the ratio of the samples that were exactly reconstructed to all 500 samples.

At this point, we should mention a fundamental difference between BP and other incorporated algorithms. OMP, SP and A*OMP (and nearly all greedy algorithms in CS) can all incorporate the

a priori information about K , the number of components in the sparse representation, and search for K -sparse representations. However, BP by its nature cannot incorporate such an information directly, and might finally produce representations that does not have exactly K components. The authors did not make any efforts to limit the number of components that BP returns, while other algorithms involved in tests return exactly K components for each signal. Note that as discussed in Section 6.4, termination criteria of A*OMP (and OMP also) can be chosen such that it does not require a priori info about K , however this formulation is not investigated in this manuscript.

7.1.1. Uniformly Distributed Coefficients

The first set of simulations employ coefficients drawn from the uniform distribution $U[-1, 1]$. The results of these simulations for K from 5 to 50 are depicted in Fig. 4 in comparison to BP, SP and OMP. We observe that the performance of the algorithms are very close in all DCT, Haar and Dirac Bases. In terms of $NMSE$, Adap-A*OMP and Mul-A*OMP clearly outperform the other algorithms. Even for $K = 35$ and $K = 40$, they promise low amounts of reconstruction error. As expected, OMP shows the worst performance in all tests. SP yields only slightly better $NMSE$. BP, which solves ℓ_1 minimization problem, provides lower error than SP and OMP, however it is still much worse than A*OMP. Even the Add-A*OMP, which employs no dynamic cost model, yields lower error than BP up to $K = 40$. In fact, we observe that reconstruction for $K \geq 45$ almost fails for all algorithms, hence comparison of the results for $K \geq 45$ do not make much sense.

On the other hand, comparison of exact reconstruction rates gives different results: Though SP results in much higher reconstruction error on average, it competes with Adap-A*OMP and Mul-A*OMP and even exceeds them at $K = 30$ when exact reconstruction rates are considered. For Add-A*OMP, the situation is contrary: It yields $NMSE$ values, which are almost equal to those of Adap-A*OMP and Mul-A*OMP until K exceeds 30, however exact reconstruction rate for Add-A*OMP is even worse than the OMP algorithm. These results indicate that Add-A*OMP can appropriately select the basis vectors with high energy contributions to \mathbf{x} , however most of the time fails at the ones with small coefficients. This is a result of the chosen auxiliary function: The assumption about the constant decay of the residue, or equivalent contribution of all K components to the energy of \mathbf{x} is an appropriate choice, with the parameter $\beta > 1$ obviously, for compensating paths at initial levels where higher energy components are involved. However at later stages, where the algorithm should restore the component with very small energy contributions, the actual energy decay per path becomes much smaller than the assumed one, reducing the accuracy on finding the most promising path. This fact increases the importance of the dynamic cost functions (adaptive and multiplicative cost models) which we propose in this manuscript, as they dynamically adjust the expected decay in the energy of the residue wrt. the actual residual energy. This fact is also clearly supported by the results provided in this section, which show that adaptive and multiplicative cost functions increase the exact reconstruction rate by large amounts, in comparison to the additive one.

Fig. 4 clearly states that $NMSE$ and exact reconstruction rates are not necessarily in parallel for all algorithms. This difference follows from the fact that algorithms approach the problem from different perspectives. Consequently, the ways they conduct errors are different from each other. Based on the results provided in this section, exact reconstruction rates of SP, Adap-A*OMP and Mul-A*OMP are close to each other. However, when SP fails, the amount of error it makes is much higher than that of the A*OMP algorithm, resulting in much higher $NMSE$ on average.

To visualize this fact, the probability density estimates of the error are depicted in Fig. 5 for SP and Mul-A*OMP. These were computed using Gaussian kernels over the test vectors which

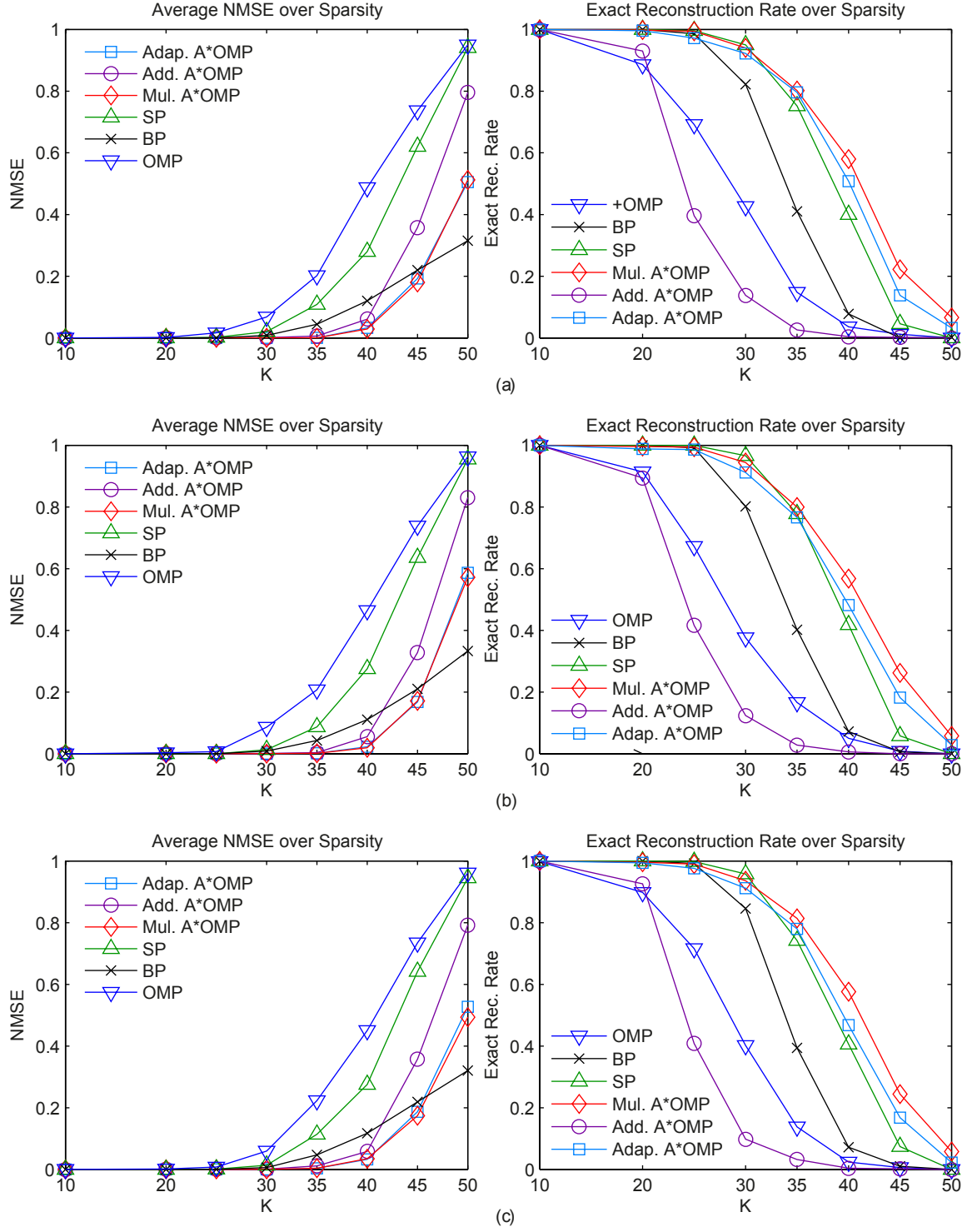


Figure 4: Average Normalized MSE and exact reconstruction rates obtained for reconstruction of sparse signals with uniform distributed coefficients in (a) DCT, (b) Haar Wavelet, and (c) Dirac bases. Simulation results are averaged over 500 test samples of length 256, each employing different Gaussian observation matrices to obtain random observations of length 100.

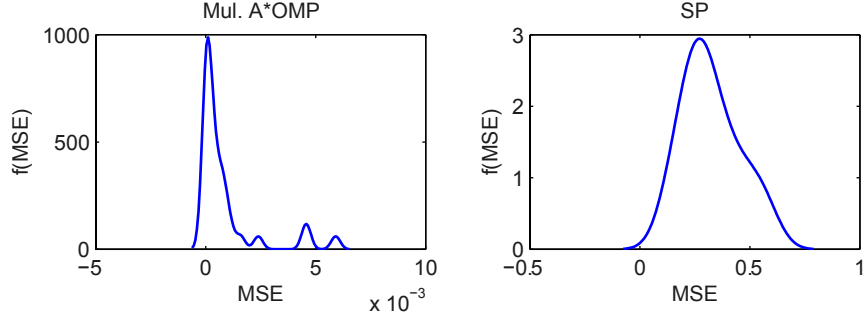


Figure 5: Probability density estimates of the NMSE after Mul-A*OMP and SP for $K = 30$ in Dirac Basis. pdf's were computed using Gaussian kernels over the K -sparse test vectors that could not be exactly reconstructed.

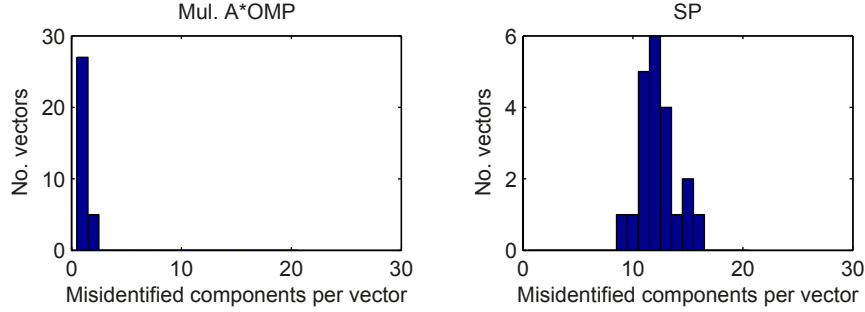


Figure 6: Histogram of the number of misidentifications per test vector for $K = 30$ in Dirac Basis. Histogram was obtained using only the vectors that could not be exactly reconstructed.

could not be exactly reconstructed for $K = 30$. The figures state that Mul-A*OMP errors lie on the order of 10^{-3} 's with mean very close to 0, while that SP range up to 0.8, with mean about 0.3. This arises from the difference in the number of misidentified elements for each erroneous reconstruction: Fig. 6 shows the histograms of the number of misidentifications per test vector for SP and Mul-A*OMP for $K = 30$. Mul-A*OMP has misidentified only one or two of the 30 components. SP, however, misses 9 to 16 components, and on average about 12 per erroneous reconstruction. These figures clearly indicate that if the reconstruction is not exact, SP almost completely fails, however A*OMP can still reconstruct the desired vector with small amount of error, which is less than 1% of the signal norm for $K = 30$.

To summarize, SP, Adap-A*OMP and Mul-A*OMP provide higher reconstruction rates than BP and OMP algorithms for uniformly distributed coefficients. In addition, Adap-A*OMP and Mul-A*OMP also provide very low reconstruction errors when the reconstruction is not exact, while SP almost completely fails. In fact, this small amount of error Adap-A*OMP and Mul-A*OMP yield is acceptable for many applications. Consequently, we conclude that Adap-A*OMP and Mul-A*OMP are superior to SP, BP and OMP for uniformly distributed coefficients.

7.1.2. Normal Distributed Coefficients

The second set of simulations was only performed in the Dirac Basis, where the nonzero entries of the sparse test vectors were drawn from the normal distribution with mean 0 and standard deviation 1. Performance of the Mul-A*OMP, SP, BP and OMP algorithms were obtained as average

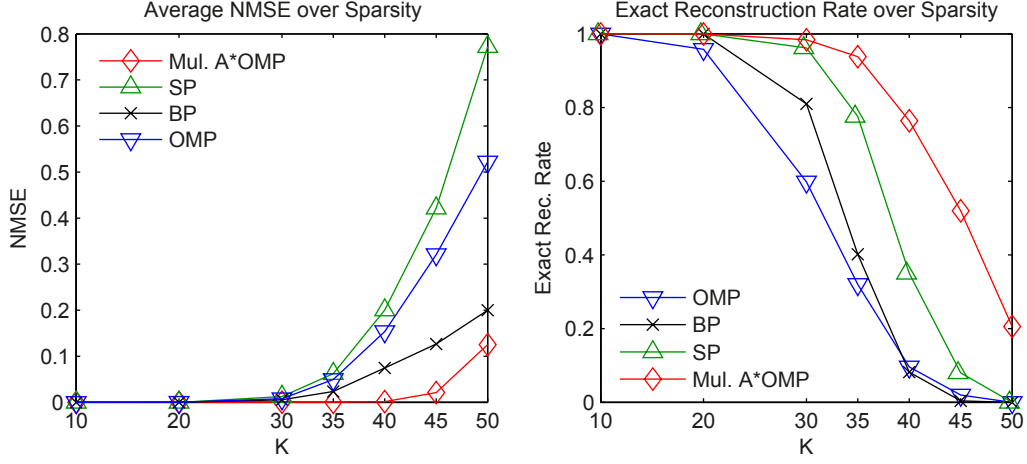


Figure 7: Average Normalized MSE and exact reconstruction rates obtained for reconstruction of sparse signals with normal distributed entries. Simulation results are averaged over 500 test samples of length 256, each employing different Gaussian observation matrices to obtain random observations of length 100.

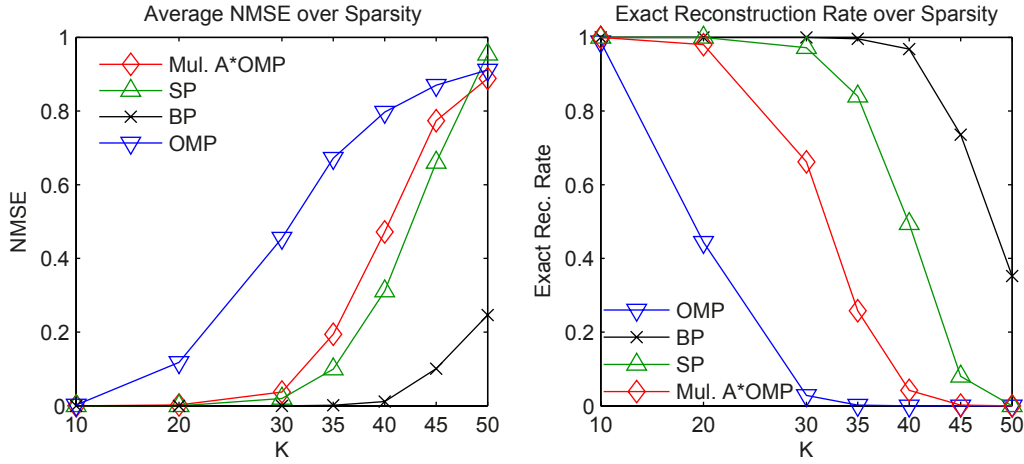


Figure 8: Average Normalized MSE and exact reconstruction rates obtained for reconstruction of sparse binary signals. Simulation results are averaged over 500 test samples of length 256, each employing different Gaussian observation matrices to obtain random observations of length 100.

over 500 test vectors as above. Fig. 7 depicts the obtained NMSE and exact reconstruction values, stating that Mul-A*OMP outperforms other three algorithms. We observe that Mul-A*OMP provides both lower NMSE and higher exact reconstruction rates than all others. Moreover, average NMSE is also smaller for Mul-A*OMP than for the other algorithms. SP yields the second best exact reconstruction rate, however, its average NMSE is the worst, as a consequence of the almost completely failing of the reconstruction when it is not exact.

7.1.3. Binary Coefficients

The last test case for the 1D reconstruction problem was obtained using the Dirac Basis by selecting the nonzero entries of the sparse vectors as 1's. The results are shown in Fig. 8. We observe that BP performs better than greedy algorithms in this binary reconstruction problem.

SP also performs better than the A*OMP. The failure of A*OMP (and other greedy algorithms) in this case is related to the fact that this case is a particularly challenging case for OMP-type of reconstruction algorithms [8]. This result states that ℓ_1 minimization is more appropriate than greedy algorithms for the sparse binary reconstruction problem. This should not, however, be discouraging since only a small portion of the real world problems can be expressed as binary.

7.2. Reconstruction of Test Images

Encouraged by the results for the synthetical data, we now simulate the reconstruction ability of A*OMP on some commonly used test images including 'Lena', 'Tracy', 'cameraman' etc. Below, we first would like to clarify how these tests were performed, in addition to some slight modifications in the algorithm. Finally, reconstruction performance will be discussed in terms of both visual and qualitative results.

Due to the nature of images, we know a priori that the DC value, i.e. the coefficient for the DC component of the basis, will generally be higher than all other coefficients, unless the image itself is very dark or very noisy. Moreover, we can safely claim that the DC component will be one of the K selected vectors for each block of the image. This a priori knowledge can be incorporated into the A*OMP algorithm by selecting the DC component for each initial path a priori. Hence, we modify the initialization process by selecting two vectors for each initial path, one of them being the DC component.

In order to reduce the complexity and memory usage, block-processing of images was performed using 8×8 blocks. This has some important advantages over processing the image as a whole. First, without block-processing, the reconstruction problem would require searching the solution among $512 \times 512 = 262144$ vectors in the holographic basis. However, block-processing reduces the problem to 4096 simplified subproblems where the holographic basis has only $N = 64$ vectors. The latter is more efficient as each vector will now be searched in a space with 4096-fold reduced dimensionality. Moreover, it is possible to process independent blocks in parallel. Second, block-processing also reduces the upper bound on the total number of paths involved in A*OMP drastically. From Section 6.2, we know that the upper bound on the number of paths evaluated by A*OMP is proportional to $I \times B^{(K-1)}$ for each K -sparse block, and $4096 \times I \times B^{(K-1)}$ in total. To illustrate, let's set $B = 2$. The upper bound on number of paths becomes $I \times 2^{(K-1)+12}$ in total, showing that reconstruction of 4096 K -sparse sub-images requires only as many paths as reconstructing a single $(K + 12)$ -sparse image. Sparse representation of the whole image, however, would require $D \gg K$ vectors, increasing the bound on the total number of paths to $I \times 2^D \gg I \times 2^{(K-1)+12}$. Finally, block-processing also reduces lengths of paths involved. As a result, block-processing decreases the complexity and memory requirements of the search.

The simulations were performed with five 512×512 grayscale images using the 2D Haar Wavelet basis. Images were first preprocessed such that each 8×8 block is K -sparse in the 2D Haar Wavelet basis, where $K = 14$, and all the results in this section were obtained using these sparse images. From each block, a measurement of length $M = 32$ was computed using the observation matrix, Φ of size 32×64 . As before, entries of Φ were modeled as iid Gaussian random variables with mean 0 and standard deviation $1/N$. Using the measurements, K -sparse representations of all blocks were reconstructed using Mul-A*OMP, Adap-A*OMP, BP, SP and OMP. Mul-A*OMP and Adap-A*OMP were run for both $B = 2$ and $B = 3$ extensions per selected path. Number of initial paths was set to $I = 3$, and the parameters of the auxiliary functions were selected as $\alpha = 0.5$ and $\beta = 1.5$ for adaptive and multiplicative cost models respectively.

Table 1: PSNR values for images reconstructed using different reconstruction algorithms

	BP	OMP	SP	Mul-A*OMP		Adap-A*OMP	
				B=2	B=3	B=2	B=3
Lena	27.5	23.6	21.5	30.2	33.3	29.5	33.4
Tracy	34.6	30.8	27.9	38	42.5	37.9	41.6
Pirate	25.7	21.7	19.3	27.5	30.5	27.4	29.1
Cameraman	28.4	24.7	22.5	32.6	36.9	31.9	35.6
Mandrill	22.3	18.4	16.1	24.1	26.7	23.5	26.8

The peak Signal-to-Noise ratio (PSNR) values obtained with the mentioned reconstruction procedure are given in Table 1. With respect to these values, A*OMP outperforms other methods. Increasing the B value from 2 to 3 further improves the recognition results. We observe that, using A*OMP instead of BP, PSNR values are increased up to 8.5 dB, which is for the image 'cameraman'. On average, A*OMP provides 6.3 dB higher PSNR on these 5 images in comparison to BP.

Fig. 9 depicts the preprocessed test image 'lena' and reconstructed images using SP, BP and Adap-A*OMP with $B = 3$. BP and Adap-A*OMP reconstructions are clearly better than SP. One can clearly see the blocks for which SP completely fails. Careful investigation of the images yields that Adap-A*OMP performs better than BP, especially around the boundaries and in detailed regions. To visualize the difference, absolute error per pixel for BP and Adap-A*OMP reconstructions is illustrated in Fig. 10. For BP, errors are concentrated around boundaries and detailed regions, such as the hair. Adap-A*OMP clearly outperforms BP, producing less distortion all around the image.

8. Conclusion

This work proposes a new algorithm, the A*OMP, for reconstruction of sparse signals from random observations in reduced dimensions. The suggested method is based on combination of the OMP with the A* search method. With this semi-greedy method, the solution of the sparse reconstruction problem can be searched over multiple paths. During the search, the paths that minimize the cost function are favored. Selection of the auxiliary function plays a crucial role for evaluating these costs. In order to find an appropriate auxiliary function, we define the additive, multiplicative and adaptive cost functions, which differ on their modeling of the expected decay of the residue. Additive cost function employs a static model, while the other two are dynamic methods.

Reconstruction performance of the A*OMP was illustrated in Section 7 on both generated signals and images. Quantitative results and reconstructed images clearly state that A*OMP outperforms BP, SP and OMP algorithms. A*OMP yields better reconstruction when using uniform and normal distributed nonzero coefficients. Under uniform distribution, it was also shown that the reconstruction performance does not depend on the basis in which the signal is sparse, and this can be generalized to other distributions as well. BP and SP perform better than A*OMP when the sparse signal is binary, however this has very limited use in real problems.



Figure 9: Reconstructions of image 'Lena' using different algorithms

Based on the promising results provided in this paper, future work on the incorporation of best-first search in compressed sensing signal recovery may be conducted on many aspects. The

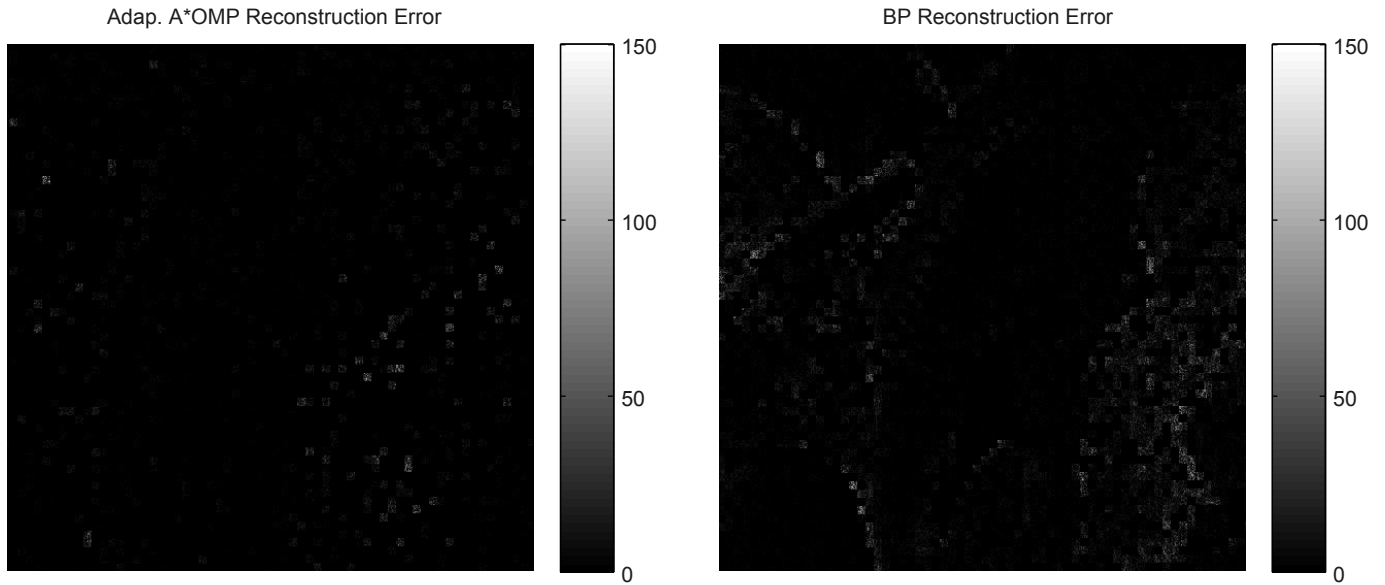


Figure 10: Reconstruction error per pixel of image 'Lena' for (a) BP reconstruction (b) Adap-A*OMP reconstruction with $B = 3$.

scheme provided in this manuscript might be used to incorporate some other cost structures, such as a dynamic multiplicative one. In addition, the OMP-based branch extension strategy may also be modified to involve some other strategies among other sparse signal reconstruction techniques.

To conclude, the demonstrated reconstruction performance of A*OMP indicates that utilization of A* search in CS reconstruction is a promising approach, that significantly reduces the reconstruction errors in realistic coefficient distributions.

References

- [1] E. Candès, J. Romberg, T. Tao, Robust uncertainty principles: Exact signal reconstruction from highly incomplete frequency information, *IEEE Trans. Inf. Theory* 52 (2) (2006) 489–509.
- [2] D. Donoho, Compressed sensing, *IEEE Trans. Inf. Theory* 52 (4) (2006) 1289–1306.
- [3] E. Candès, T. Tao, Near-optimal signal recovery from random projections: universal encoding strategies?, *IEEE Trans. Inf. Theory* 52 (12) (2006) 5406–5425.
- [4] S. Chen, D. Donoho, M. Saunders, Atomic decomposition by basis pursuit, *SIAM J. on Sci. Comp.* 20 (1) (1998) 33–61.
- [5] S. Mallat, Z. Zhang, Matching pursuit in a time-frequency dictionary, *IEEE Trans. Signal Process.* 41 (12) (1993) 3397–3415.
- [6] Y. C. Pati, R. Rezaiifar, P. S. Krishnaprasad, Orthogonal matching pursuit: Recursive bfunction approximation with applications to wavelet decomposition, in: *Proc. 27th Asilomar Conference on Signals, Systems and Computers*, Vol. 1, Los Alamitos, CA, 1993, pp. 40–44.
- [7] D. Needell, R. Vershynin, Uniform uncertainty principle and signal recovery via regularized orthogonal matching pursuit, *Found Comput Math* 9 (3) (2009) 317–334.
- [8] W. Dai, O. Milenkovic, Subspace pursuit for compressive sensing signal reconstruction, *IEEE Trans. Inf. Theory* 55 (5) (2009) 2230–2249.
- [9] D. Needell, J. A. Tropp, CoSaMP: Iterative signal recovery from incomplete and inaccurate samples, *Appl. Comp. Harmonic Anal.* 26 (2008) 301–321.
- [10] S. Koenig, M. Likhachev, Y. Liu, D. Furcy, Incremental heuristic search in ai, *AI Mag.* 25 (2) (2004) 99–112.
- [11] R. Dechter, J. Pearl, Generalized best-first search strategies and the optimality of A*, *J. ACM* 32 (3) (1985) 505–536. doi:<http://doi.acm.org/10.1145/3828.3830>.

- [12] F. Jelinek, Statistical Methods For Speech Recognition, MIT Press, Cambridge, MA, USA, 1997, Ch. 6.
- [13] P. E. Hart, N. J. Nilsson, B. Raphael, A formal basis for the heuristic determination of minimum cost paths, *IEEE Trans. Syst. Sci. Cybern.* 4 (12) (1968) 100–107.
- [14] P. E. Hart, N. J. Nilsson, B. Raphael, Correction to a formal basis for the heuristic determination of minimum cost paths, *SIGART Newsletter* (37) (1972) 28–29.
- [15] N. B. Karahanoglu, H. Erdogan, Compressed sensing signal recovery via a* orthogonal matching pursuit, in: *Acoustics, Speech and Signal Processing (ICASSP)*, 2011 IEEE International Conference on, 2011, pp. 3732–3735.
- [16] M. Wakin, Compressed sensing, *Connexions* (Sep. 2009).
URL <http://cnx.org/content/m18733/1.5/>
- [17] E. Candès, M. Rudelson, T. Tao, R. Vershynin, Error correction via linear programming, in: *Proceedings of the 46th Annual IEEE Symposium on Foundations of Computer Science (FOCS)*, Pittsburgh, PA, 2005, pp. 295–308.
- [18] J. A. Tropp, S. J. Wright, Computational methods for sparse solution of linear inverse problems, *Proc. IEEE* 98 (6) (2010) 948–958. doi:10.1109/JPROC.2010.2044010.
- [19] S. S. Chen, Basis pursuit, Ph.D. thesis, Stanford University, Stanford, CA (Nov. 1995).
- [20] E. Candès, T. Tao, Decoding by linear programming, *IEEE Trans. Inf. Theory* 51 (12) (2005) 4203–4215.
- [21] E. Candès, The restricted isometry property and its implications for compressed sensing, *Comptes Rendus Mathématique* 346 (9–10) (2008) 589–592.
- [22] J. A. Tropp, A. C. Gilbert, Signal recovery from random measurements via orthogonal matching pursuit, *IEEE Trans. Inf. Theory* 53 (12) (2007) 4655–4666.
- [23] M. Rudelson, R. Vershynin, Sparse reconstruction by convex relaxation: Fourier and gaussian measurements, in: *40th Annual Conference on Information Sciences and Systems*, 2006, pp. 207–212.